Hindawi
Advances in Civil Engineering
Volume 2019, Article ID 4328103, 9 pages
https://doi.org/10.1155/2019/4328103

Research Article

Model Test Study on the Antibreaking Technology of Reducing Dislocation Layer for Subway Interval Tunnel of the Stick-Slip Fracture

Guang-yao Cui and Xue-lai Wang

School of Civil Engineering, North China University of Technology, Beijing 100144, China

Correspondence should be addressed to Xue-lai Wang; jjlam124@163.com

Received 3 June 2019; Accepted 13 September 2019; Published 7 October 2019

Academic Editor: Tayfun Dede

Based on the background of the Line $F_{2\text{-}3}$ interval tunnel section of Jiujiawan in Urumqi Subway Line 1, this paper carries out the model test research on the antibreaking technology of the reducing dislocation layer in the tunnel section of the stick-slip fracture. The antibreaking effect of different locations and number of reducing dislocation layers in tunnel engineering is analyzed in this paper. The results show that when the double reducing dislocation layer, respectively, set between the surrounding rock and the primary support, and the primary support and the secondary lining, the antibreaking effect is the best. It is recommended to use this scheme for antibreaking design. The research results can provide reference for antibreaking design of traffic tunnels in active fault zones.

1. Introduction

A great quantity of cities in the world are built on fault zones, so in the process of tunnel construction, there will inevitably be many cross-fault tunnels [1]. With the continuous and deep development of the construction of traffic infrastructure in China, the traffic tunnelling projects in active fault areas are constantly emerging, such as the Lasa-Rikaze series tunnel crossing Yajiang deep fault and Yajiang north shore fault, the Sichuan-Tibet series tunnel crossing Longmen Hill, Xianshui River, Woka, Basu, and other faults, the Erlangshan tunnel of the Yaan-Kangding highway crossing Luding, Erlangshan, Baohuang, and other faults, the Lanjiayan tunnel of the Mianzhu-Maoxian highway crossing the Longmen mountain branch fracture, and the Urumqi Subway Line 1 crossing Bagangshihua, Jiujiawan, Xishan, Yamalike Mountain, and other faults (see Figure 1).

Strong earthquakes induce stick-slip dislocation of active faults, which is the main cause of serious damage to the tunnel structure [2–4]. How to improve the antibreaking performance of the tunnel with the stick-slip fracture is one of the key technical problems to be studied and solved urgently.

Experts and scholars all over the world have carried out some researches on the antibreaking technology of the traffic tunnel with the stick-slip fracture, which mainly includes the following aspects: the mechanical response, failure, and damage mechanism of the tunnel structure and surrounding rock under the fault stick-slip dislocation based on the interaction were studied by model test and numerical simulation [5–10]. Relying on the Bolu tunnel in Turkey and the Koohrang hydraulic tunnel in Greece, the effect of the reducing dislocation joint on the secondary lining with different pitches was compared [11, 12]. The model test was used to study the mechanical response and the antibreaking effect of the reducing dislocation joint on the secondary lining [13, 14]. The model test and theoretical analysis were used to study the damping model, the absorption mechanism, and the sensitivity of the parameters [1, 15].

To sum up, there were more researches on the antibreaking technology of the reducing dislocation joint for the secondary lining of the stick-slip fracture tunnel at

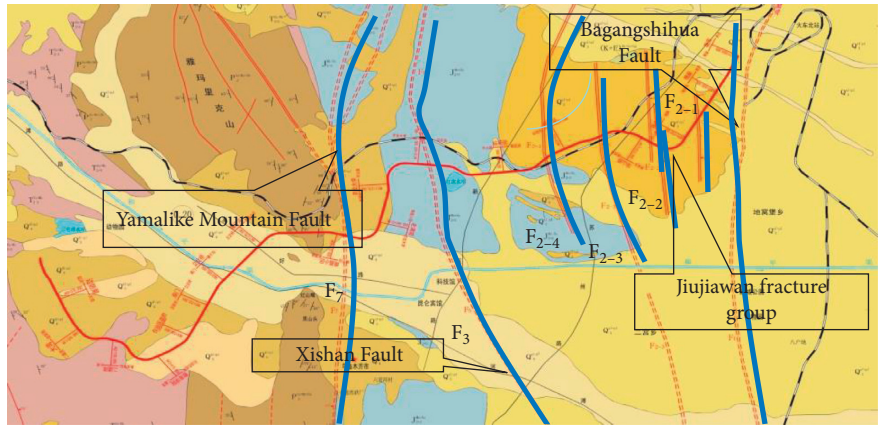

Figure 1: Geotecture of the region of Urumqi Subway Line 1.

present. However, few studies to date have investigated the antibreaking technology of the reducing dislocation layer. Based on the background of the Line $F_{2\text{-}3}$ interval tunnel section of Jiujiawan in Urumqi Subway Line 1, this paper designs several sets of model test. The purpose of this paper is to study in detail the antibreaking measures of the reducing dislocation layer in the stick-slip fracture tunnel, which is of great significance to the improvement of the structural safety and stability of the traffic tunnel in the active fault zones.

2. The Overview of Urumqi Subway Line 1

2.1. Project Overview. The Urumqi Subway Line 1 starts in Santunbei and ends at the airport. The total length of the line is 26.5 km, and a total of 21 underground stations are set up. The average distance between the stations is 1.3 km.

2.2. Main Active Faults. The Urumqi Subway Line 1 passes through the Yamalike Mountain Fault (F_7), the Bayi Petrochemical Concealed Fault (F_1), the Jiujiawan Fault (F_2), and the Xishan Fault (F_3) from south to north. The basic condition of the fracture is shown in Table 1.

2.3. Structure Design of Interval Tunnel. The cross section of the subway tunnel is horseshoe-shaped with a span of 8.573 m and a height of 9.120 m. The thickness of the primary support is 30 cm, which is C25 shotcrete [16], and the thickness of the secondary lining is 60 cm, which is C30 cast concrete.

3. Test Scheme Design

3.1. Test Grouping. In order to study the antibreaking effect of the different locations of the reducing dislocation layer of the stick-slip fracture tunnel, four groups of indoor model tests have been carried out, and the thickness of the reducing dislocation layer is 10 cm [15]. The test grouping is shown in Table 2.

3.2. Test Equipment and Similarity Ratio Design. The test was carried out by a self-designed leaning straight stick-slip dislocation test box. The test box is composed of a movable hanging wall and a fixed footwall, and the fracture angle is 70°. The size of the test box is long∗wide∗high = 2.5 m∗2.5 m∗2 m (see Figure 2).

The test sensors are made of strain gauges, rectangular rosette, and miniature pressure boxes (see Figure 3). Donghua static strain acquisition instrument is used to collect data.

Considering the size of the test box, the size of the tunnel, and the effect of the boundary, the geometric similarity ratio is 30. Considering the similar matching of severity between the actual material and similar materials, the similarity ratio of the modulus of elasticity is 45. The acceleration similarity ratio is 1. According to the similarity theory, the similarity ratio of other related physical quantities is shown in Table 3.

3.3. Test Similarity Materials. Through the orthogonal test, the way of determining the weight ratio of each component is by the similar material of the surrounding rock, and the ratio is machine oil : river sand : fly ash = 1 : 3 : 6. Basic mechanical parameters of similar materials in surrounding rock are shown in Table 4.

The test used the gypsum admixture to simulate the secondary lining, and the water-paste ratio of gypsum admixture is 0.641. Similar control indexes are elastic modulus and compressive strength. Through the equivalent principle of bending stiffness, a steel wire with a specific diameter is used to simulate the main bar of the secondary lining. The primary support is simulated by gypsum. The foamed rubber plate of 3.6 mm thick is used to simulate the reducing dislocation layer. Polyethylene film was used to simulate the waterproof board. The two layers of PVC plastic plate, evenly coated with butter in the middle, is used to simulate the effect of stick-slip dislocation (see Figure 4).

3.4. Measurement Arrangement of Testing. Measurement arrangement of testing is as shown in Figure 5. Miniature pressure box (Y, set up between surrounding rock and primary

Table 1: Condition of activity and breaking of Urumqi Subway Line 1.

Name of fracture	Fracture properties	Dip (°)
Bagangshihua	Late Pleistocene active reverse fault	75
The $F_{2\text{-}1}$ of Jiujiawan	Holocene active normal fault	80
$F_{2\text{-}2}$ North Branch of Jiujiawan	Holocene active normal fault	50
$F_{2\text{-}2}$ South Branch of Jiujiawan	Holocene active normal fault	70
The F_3 of Jiujiawan	Holocene active normal fault	70
The F_4 of Jiujiawan	Holocene active normal fault	60
North Branch of Xishan	Late Pleistocene active reverse fault	45
South Branch of Xishan	Late Pleistocene active reverse fault	45
Yamalike mountain	Late Pleistocene active reverse fault	70

Table 2: Test grouping.

Working condition	Test contents
1	No antibreaking measures
2	The single reducing dislocation layer set between the surrounding rock and the primary support
3	The single reducing dislocation layer set between the secondary lining and the primary support
4	The double reducing dislocation layer respectively set between the surrounding rock and the primary support and between the primary support and the secondary lining.

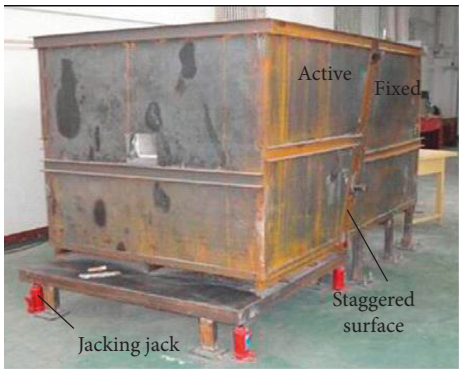

Figure 2: Leaning straight stick-slip dislocation test box.

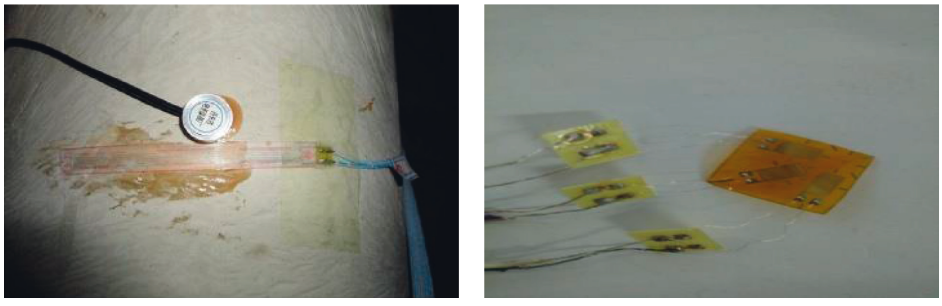

(a) (b)

Figure 3: Test sensor. (a) Miniature pressure boxes. (b) Rectangular rosette.

support) was arranged in the vault, the middle of the side wall, and the middle of the inverted arch, and transverse strain gauges (H, set in pairs on the inside and outside of the secondary lining), longitudinal strain gauges (L, set on the outer side of the secondary lining), and right angle strain flowers (Z, set on the outer side of the secondary lining) were arranged on the vault.

Table 3: Similarity ratio of other related physical quantities.

Physical quantity	Similarity ratio
Strain/Poisson ratio/internal friction angle/angular displacement	1
Bulk density	1.5
Stress/cohesion	45
Area	900
Load	40,500
Moment	1,215,000

Table 4: Basic mechanical parameters of similar materials in surrounding rock.

Parameter	Modulus of elasticity (MPa)	Bulk density (kN·m^{-3})	Cohesive (kPa)	Internal friction angle (°)
Archetypal surrounding rock	1300~6000	17~20	20~200	20~27
Tunnel rock similar material	29.6	12.6	3.3	24.5

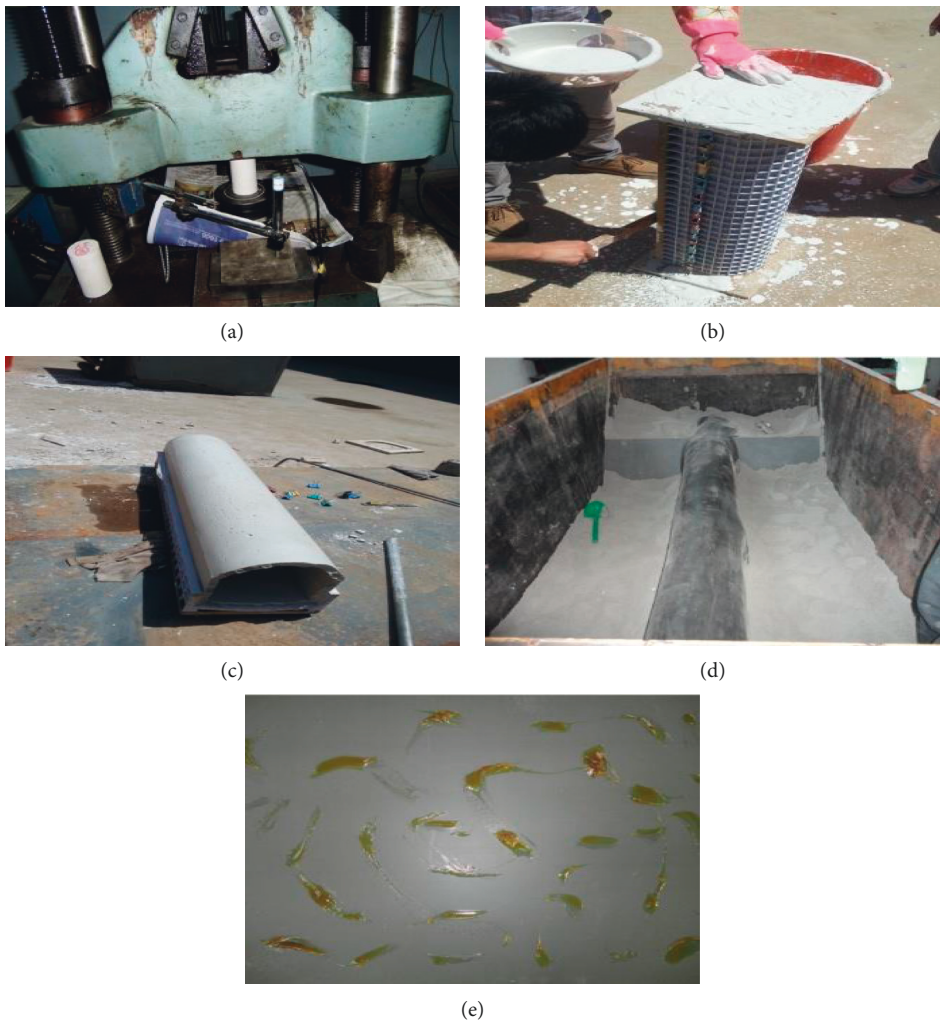

Figure 4: Test similar material. (a) Mechanical testing of lining similar materials. (b) Secondary lining model pouring. (c) Dismantling of the secondary lining model. (d) Foamed rubber plate simulating the reducing dislocation layer. (e) Simulation of the stick-slip fracture.

3.5. Test Process. Firstly, the jacks at the bottom corners of the upper part of the test box were raised by 5 cm (according to the requirement of engineering life of 100 years, the conservative prediction of surface dislocation momentum is 1.5 m). Secondly, the similar materials of the surrounding rock were filled to the bottom of the tunnel model at a height of 0.2 m per raft, and the secondary lining was laid. The model, the waterproof board and the reducing dislocation layer, and the sensor were installed.

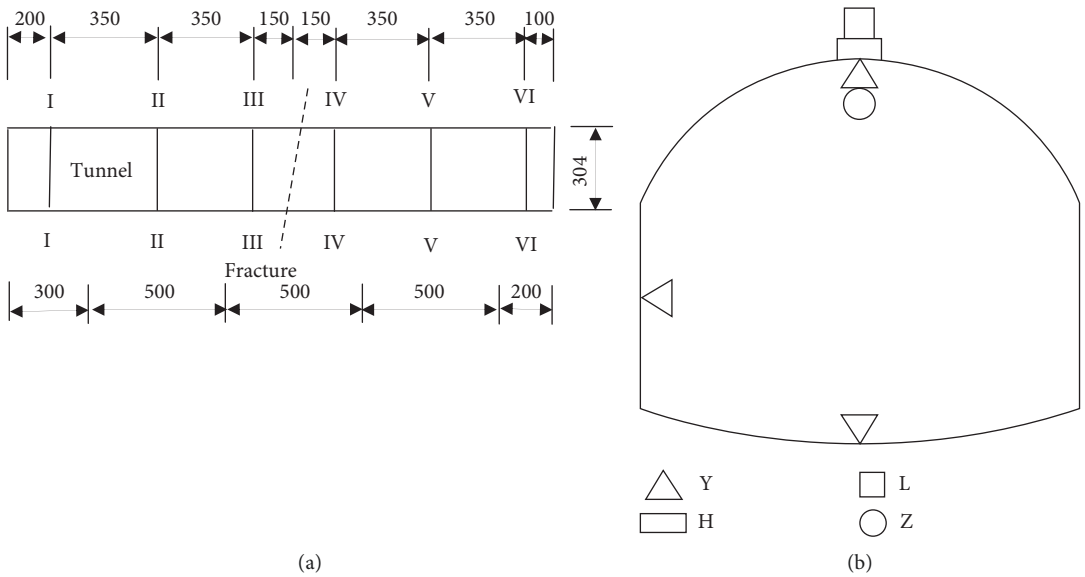

Figure 5: Arrangement of the testing section and measuring points. (a) Measuring section (unit: mm). (b) Arrangement of measuring points.

Finally, the similar materials of the surrounding rock were filled to the surface elevation, the four jacks at the bottom of the upper plate were simultaneously lowered, the upper plate was viscous-slip along the fracture surface, and the test was completed.

4. Test Data and Analysis

4.1. Principal Stress. After the test, the test data of the rectangular rosette of each section of the each working condition were extracted to calculate the principal stress of the structure caused by the stick-slip fracture (see Figure 6). The hanging wall is the positive part of the abscissa, and the footwall is the negative part of the abscissa.

The principal stress of each working condition was extracted, and the antibreaking effect was calculated, as shown in Table 5.

As shown in Figure 6 and Table 5,

(1) After the stick-slip dislocation, the first principal stress and the third principal stress of the hanging wall tunnel are obviously larger than the part of the footwall tunnel.

(2) After applying the reducing dislocation layer, the principal stress changes from a more drastic change to a more uniform change in the longitudinal direction of the tunnel.

(3) The antibreaking effect of the principal stress of working condition 2, the single reducing dislocation layer was set between the surrounding rock and the primary support and is better than working condition 3. The single reducing dislocation layer was set between the secondary lining and the primary support. When the single reducing dislocation layer is applied between the surrounding rock and the primary support, the antibreaking effect of the principal stress is 40% to 50%, and when it is applied between the primary support and the secondary lining, the antibreaking effect of the principal stress is 30% to 40%.

(4) In working condition 4, that is, when the double reducing dislocation layer is respectively applied between the surrounding rock and the primary support and between the primary support and the secondary lining, the main stress has the best antibreaking effect, which is 60% to 70%.

4.2. Longitudinal Strain. After the test, the test data of the longitudinal strain gauge of each section of the each working condition were extracted to calculate the increasing multiples of the longitudinal strain of the structure caused by the stick-slip fracture (see Figure 7).

The maximum value of increasing multiple of longitudinal strain of each working condition was extracted, and the antibreaking effect was calculated (see Table 6).

As shown in Figure 7 and Table 6,

(1) After the stick-slip dislocation, the increasing multiple of longitudinal strain of the hanging wall tunnel is obviously larger than the part of the footwall tunnel.

(2) After applying the reducing dislocation layer, the increasing multiple of longitudinal strain changes from a more drastic change to a more uniform change in the longitudinal direction of the tunnel.

(3) The antibreaking effect of the longitudinal strain of working condition 2 is 97.89%, which is slightly better than working condition 3, which is 97.86%. Working condition 4 has the best longitudinal strain antibreaking effect, which is 98.55%.

4.3. Contact Pressure. After the test, the test data of the miniature pressure box of each section of each working

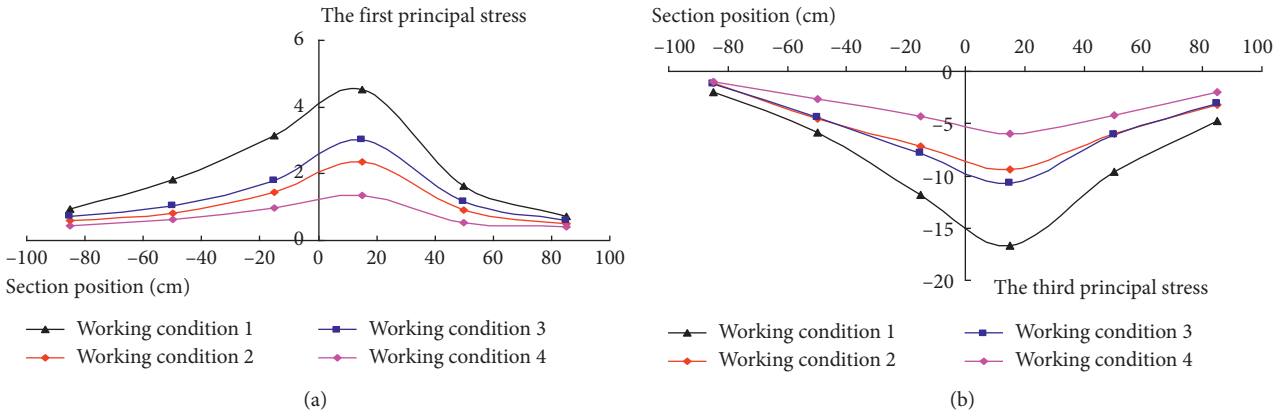

Figure 6: Principal stress. (a) The first principal stress. (b) The third principal stress.

Table 5: The antibreaking effect of principal stress.

Working conditions	The maximum value of the first principal stress (MPa)	The antibreaking effect of the first principal stress (%)	The maximum value of the third principal stress (MPa)	The antibreaking effect of the third principal stress (%)
1	4.54	—	16.72	—
2	2.36	48.11	9.36	44.04
3	3.01	33.70	10.71	35.96
4	1.37	69.82	6.01	64.06

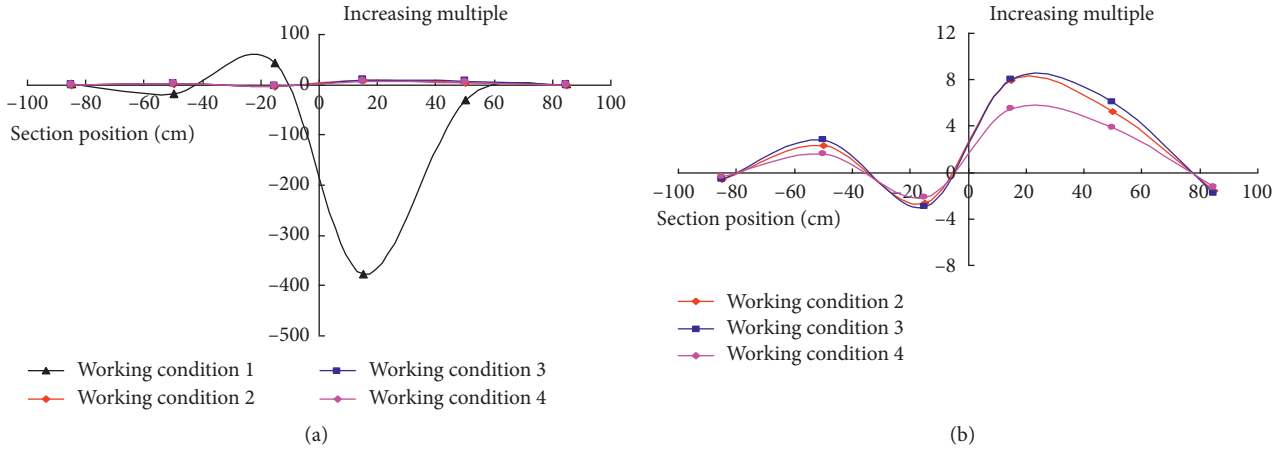

Figure 7: Increasing multiple of longitudinal strain. (a) Working conditions 1 to 4. (b) Working conditions 2 to 4.

Table 6: Antibreaking effect of longitudinal strain.

Working conditions	The maximum value of increasing multiple of longitudinal strain	The antibreaking effect
1	376.39	—
2	7.96	97.89
3	8.06	97.86
4	5.46	98.55

condition were extracted to calculate the increasing multiples of the contact pressure of the structure caused by the stick-slip fracture (see Figure 8).

The maximum value of increasing multiple of contact pressure of each working condition was extracted, and the antibreaking effect was calculated (see Table 7).

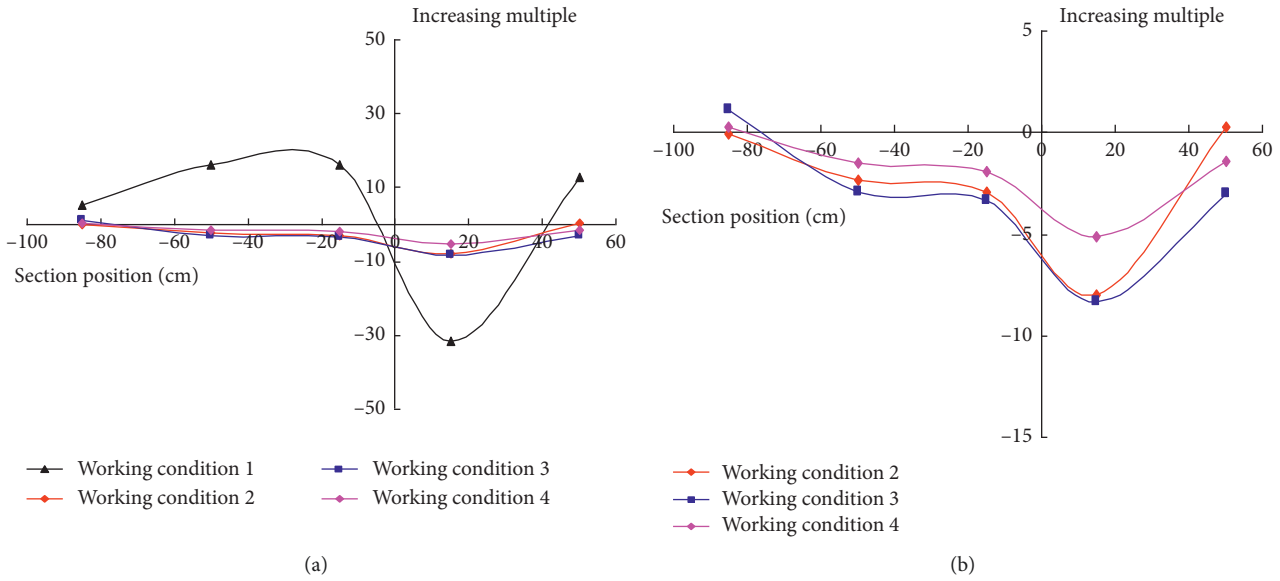

Figure 8: Increasing multiple of contact pressure. (a) Working conditions 1 to 4. (b) Working conditions 2 to 4.

Table 7: Antibreaking effect of contact pressure.

Working conditions	The maximum value of increasing multiple of contact pressure	The antibreaking effect (%)
1	31.76	—
2	7.96	74.92
3	8.36	73.69
4	5.42	82.93

As shown in Figure 8 and Table 7,

(1) After the stick-slip dislocation, the increasing multiple of contact pressure of the hanging wall tunnel is obviously larger than the part of the footwall tunnel.

(2) After applying the reducing dislocation layer, the increasing multiple of contact pressure changes from a more drastic change to a more uniform change in the longitudinal direction of the tunnel.

(3) The antibreaking effect of the contact pressure of working condition 2 is 74.92%, which is slightly better than working condition 3, which is 73.69%. The contact pressure of working condition 4 has the best antibreaking effect, which is 82.93%.

4.4. Structural Internal Forces. The axial force, bending moment, and safety factor value of the structure are calculated by measuring the lateral strain gauge of the inner and outer side of the vault of each section of each working condition [17, 18] (see Figure 9).

The axial force and bending moment of lining are

$$N = \frac{1}{2}E\left(\varepsilon_{\text{inside}} + \varepsilon_{\text{outside}}\right)bh,$$
$$M = \frac{1}{12}E\left(\varepsilon_{\text{inside}} - \varepsilon_{\text{outside}}\right)bh^2. \quad (1)$$

Safety factor of lining is

$$KN \le \phi\alpha R_a bh,$$
$$KN \le \phi\frac{1.75R_l bh}{6e_0/h - 1}. \quad (2)$$

In the formula, the width of the section is expressed by b and the width of the section is 1 m. The thickness of the section is expressed by h. The modulus of elasticity is expressed in E. The internal and external strain of the structure is expressed by $\varepsilon_{\text{inside}}$ and $\varepsilon_{\text{outside}}$, respectively. The structural axial force is expressed by N. The bending moment is expressed by M. The ultimate compressive strength of concrete is expressed by R_a. The ultimate tensile strength of concrete is expressed by R_l. The safety factor is expressed by K. The longitudinal bending coefficient of components is expressed by ϕ. The influence coefficient of axial force eccentricity is expressed by α.

The minimum value of the safety factor of each working condition is extracted, and the increasing multiple of the minimum value is calculated (see Table 8).

As shown in Figure 9 and Table 8,

(1) After the stick-slip dislocation, the structural safety factor of the hanging wall tunnel is obviously larger than the part of the footwall tunnel.

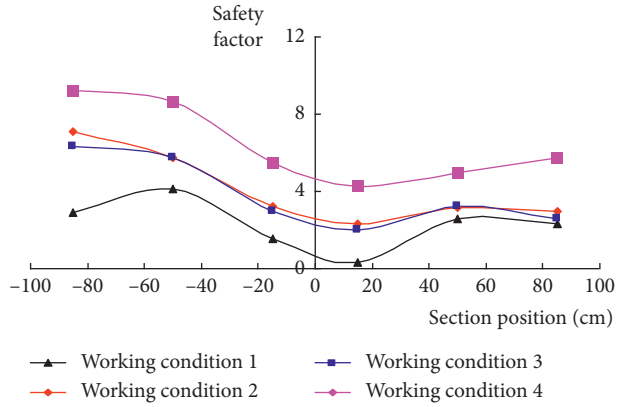

Figure 9: Safety factor of the tunnel vault.

Table 8: Increasing multiple of the minimum value of the safety factor.

Working conditions	The minimum value of the safety factor	The increasing multiplier
1	0.33	—
2	2.30	6.98
3	2.01	6.10
4	4.26	12.91

(2) The increasing multiple of the minimum value of the structural safety factor of working condition 2 is 6.98 times, which is slightly greater than working condition 3, which is 6.10 times. This shows that antibreaking effects of the project of the single reducing dislocation layer, set between the surrounding rock and the primary support, is slightly better than that of the single reducing dislocation layer, set between the primary support and the secondary lining.

(3) The increasing multiple of the minimum value of the structural safety factor of working condition 4 is the maximum, which is 12.91 times. The minimum value of the structural safety factor is 4.26, and it meets the structural safety requirements of the project for a hundred years of conservative prediction of the dislocation. It is recommended to use this scheme for the antibreaking fortification design, namely, the project of the double reducing dislocation layer, respectively set between the surrounding rock and the primary support and the primary support and the secondary lining.

5. Conclusion

(1) After applying the reducing dislocation layer, the increasing multiple of the structural principal stress, longitudinal strain, and contact pressure changes from a more drastic change to a more uniform change in the longitudinal direction of the tunnel.

(2) When single reducing dislocation layer is laid between surrounding rock and primary support, the antibreaking effect of principal stress, longitudinal strain, contact pressure, and structural internal force is slightly better than that when single reducing dislocation layer is laid between primary support and secondary lining.

(3) The antibreaking effect of the project of double reducing dislocation layer, respectively, set between the surrounding rock and the primary support and between the primary support and the secondary lining is the best. The antibreaking effect of the principal stress is 60% to 70%, the antibreaking effect of the longitudinal strain is 98.55%, and the antibreaking effect of the contact pressure is 82.93%. The minimum value of the structural safety factor is 4.26, and the increase of its multiplier is 12.91 times, and it meets the structural safety requirements of the project for a hundred years of conservative prediction of the dislocation, so it is recommended to use for the antibreaking fortification design.

Data Availability

The data used to support the findings of this study are included within the article.

Conflicts of Interest

The authors declare that there are no conflicts of interest regarding the publication of this paper.

Acknowledgments

The authors appreciate the support from the National Natural Science Foundation of China (nos. 51408008 and 51478277).

References

[1] M. H. Baziar, A. Nabizadeh, C. J. Lee, and W. Y. Hung, "Centrifuge modeling of interaction between reverse faulting and tunnel," *Soil Dynamics and Earthquake Engineering*, vol. 65, pp. 151–164, 2014.

[2] S. Ardeshiri-Lajimi, M. Yazdani, and A. A. Langroudi, "Control of fault lay-outs in seismic design of large underground caverns," *Tunneling and Underground Space Technology*, vol. 50, pp. 305–316, 2015.

[3] M. H. Baziar, A. Nabizadeh, R. Mehrabi, C. J. Lee, and W. Y. Hung, "Evaluation of underground tunnel response to reverse fault rupture using numerical approach," *Soil Dynamics and Earthquake Engineering*, vol. 83, pp. 1–17, 2016.

[4] Y. Haitao, J. Chen, A. Bobet, and Y. Yuan, "Damage observation and assessment of the Longxi tunnel during the Wenchuan earthquake," *Tunneling and Underground Space Technology*, vol. 54, pp. 102–116, 2016.

[5] A. G. Chermahini and H. Tahghighi, "Numerical finite element analysis of underground tunnel crossing an active reverse fault: a case study on the Sabzkouh segmental tunnel," *Geomechanics and Geoengineering*, vol. 14, no. 3, pp. 155–166, 2019.

[6] Z. Z. Wang and C. Chen, "Fuzzy comprehensive Bayesian network-based safety risk assessment for metro construction projects," *Tunnelling and Underground Space Technology*, vol. 70, pp. 330–342, 2017.

[7] X. Liu, X. Li, Y. Sang, and L. Lin, "Experimental study on normal fault rupture propagation in loose strata and its impact on mountain tunnels," *Tunnelling and Underground Space Technology*, vol. 49, pp. 417–425, 2015.

[8] Z. Z. Wang, Y.-J. Jiang, C. A. Zhu, and T. C. Sun, "Shaking table tests of tunnel linings in progressive states of damage," *Tunnelling and Underground Space Technology*, vol. 50, pp. 109–117, 2015.

[9] X. Liu, X. Wang, and L. Lin, "Model experiment on effect of normal fault with 75° dipangle stick-slip dislocation on highway tunnel," *Chinese Journal of Rock Mechanics and Engineering*, vol. 32, no. 8, pp. 1714–1720, 2013.

[10] W. W. Sim, I. Towhata, S. Yamada, and G. J.-M. Moinet, "Shaking table tests modelling small diameter pipes crossing a vertical fault," *Soil Dynamics and Earthquake Engineering*, vol. 35, pp. 59–71, 2012.

[11] M. Russo, G. Germani, and W. Amberg, "Design and construction of large tunnel through active faults: a recent application," in *Proceedings of the International Conference of Tunneling and Underground Space Use*, pp. 16–18, Istanbul, Turkey, October 2015.

[12] A. R. Shahidi and M. Vafaeian, "Analysis of longitudinal profile of the tunnels in the active faulted zone and designing the flexible lining (for Koohrang-III tunnel)," *Tunneling and Underground Space Technology*, vol. 20, no. 3, pp. 213–221, 2015.

[13] Z. Z. Wang, Y. J. Jiang, and C. A. Zhu, "Seismic energy response and damage evolution of tunnel lining structures," *European Journal of Environmental and Civil Engineering*, vol. 23, no. 6, pp. 758–770, 2019.

[14] X. Liu, J. Liu, X. Li, and G. Chen, "Experimental research on effect of anti-dislocation of highway tunnel lining with hinge joints in thrust fault," *Chinese Journal of Rock Mechanics and Engineering*, vol. 34, no. 10, pp. 2083–2090, 2015.

[15] M.-N. Wang and G. Cui, "Establishment of tunnel damping model and research on damping effect with model test in highly seismic area," *Rock and Soil Mechanics*, vol. 31, pp. 1884–1890, 2010.

[16] Ministry of Housing and Urban-Rural Construction of the People's Republic of China, *GB 50010-2010 Code for Design of Concrete Structures*, Ministry of Housing and Urban-Rural Construction of the People's Republic of China, Beijing, China, 2010, in Chinese.

[17] China Architecture & Building Press, *GB50157-2013 Code for Design of Metro*, China Architecture & Building Press, Beijing, China, 2013, in Chinese.

[18] China Communications Press, *JTG D70-2004 Code for Design of Road Tunnel*, China Communications Press, Beijing, China, 2004, in Chinese.